



LABORATORI NAZIONALI DI FRASCATI
SIS – Pubblicazioni

LNF-95/063 (IR)
7 Dicembre 1995

Mode Analysis of Laser-Interferometric Gravitational Wave Detectors

D. Babusci, H. Fang, G. Giordano, G. Matone, L. Matone, V. Sannibale

INFN – Laboratori Nazionali di Frascati, P.O. Box 13, I 00044-Frascati (Roma) Italy

Abstract

A mode analysis of the VIRGO gravitational wave detector is presented. The dark fringe condition and the background at the detector have been examined. The plane-parallel and the plano-concave configurations for the recycling cavities have been compared. No substantial differences have been envisaged.

PACS.: 04.80.+z; 07.60.Ly

Introduction

The VIRGO laser-interferometric gravitational-wave (GW) detector is a Michelson interferometer with Fabry-Perot (FP) cavities in each arm and with a recycling mirror to improve the signal to noise ratio. The recycling technique has been studied extensively, [1], [2], [3], [4], but the transverse mode effects on the recycling performance have been seldom considered. Since the separations between the interferometer mirrors are much larger than the mirror sizes, the diffraction effects play an important role, and the use of the plane wave approximation for the whole interferometer is not quite satisfactory. Since each optical resonator has its own eigenmodes, a poor transverse mode matching among the input laser beam, the recycling cavities, and the FP cavities may worsen the detection sensitivity of the interferometer.

1 Optical Resonator Descriptions

The VIRGO interferometer contains two FP cavities in each Michelson arm, and two recycling cavities which have a common recycling mirror M_0 at the input beam line as shown in Fig. 1.

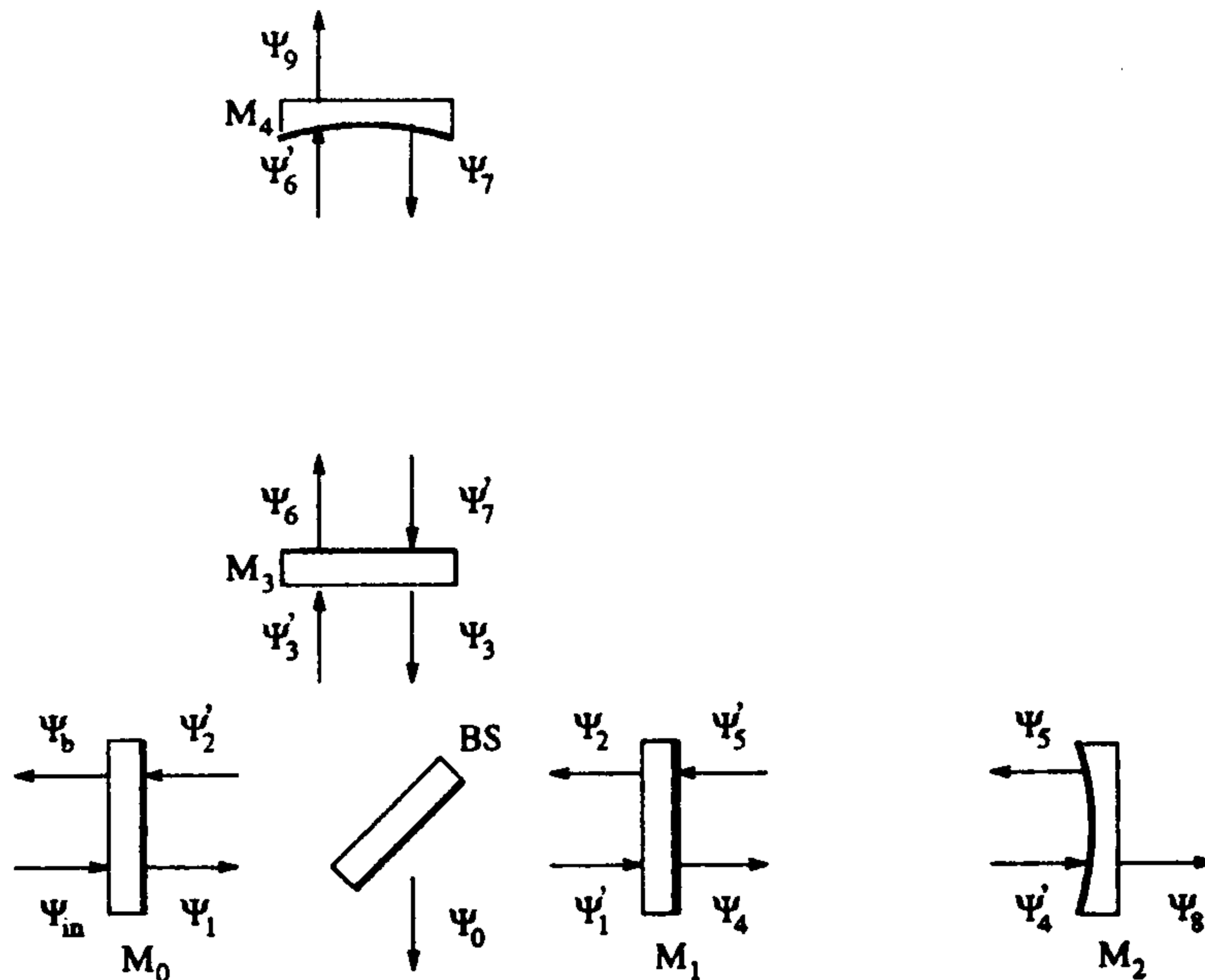


Figure 1: VIRGO Interferometer

For the sake of simplicity all the mirrors will be assumed square with size $2a$. The mirrors M_1 , M_2 are identical to the mirrors M_3 and M_4 . The two FP resonators are plano-concave and the recycling cavities may be plane-parallel or plano-concave.

For any nonsymmetric resonators the cavity modes at the left mirror, $E_{mn}^L(x, y)$, are related to the cavity modes at the right mirror, E_{mn}^R , by the following equations [5]

$$\gamma_{mn}^L E_{mn}^L(x, y) = \int \int_{M^R} K^R(x, y; x', y') E_{mn}^R(x', y') dx' dy' \quad (1)$$

$$\gamma_{mn}^R E_{mn}^R(x, y) = \int \int_{M^L} K^L(x, y; x', y') E_{mn}^L(x', y') dx' dy' \quad (2)$$

where $K^L(x, y; x', y')$ and $K^R(x, y; x', y')$ are the integral kernels of the resonator in the two directions, see [5]; the integrals are taken over the corresponding mirror surfaces M^R and M^L ; m, n are the (x, y) transverse mode indices and $\gamma_{mn}^L, \gamma_{mn}^R$ yield the round-trip eigenvalues

$$\gamma_{mn} = \gamma_{mn}^L \gamma_{mn}^R = \Gamma_{mn} \exp[-i(2kL - \phi_{mn})] \quad (3)$$

where $L_{mn} = 1 - \Gamma_{mn}^2$ are the so-called diffraction losses, and ϕ_{mn} are the Guoy phases, which are additional phase shifts due to the finite transverse beam size and depend on the specific cavity configuration. The resonance frequency is determined by the equation

$$\Delta_{mn} = 2kL - \phi_{mn} = 2q\pi \quad (4)$$

where L is the separation of the cavity mirrors, q is an integer, and $k = \frac{2\pi}{\lambda}$.

2 Mode Analysis of the Interferometer

In the configuration shown in Fig. 1, we assume that the separations between M_1 and M_2 , M_3 and M_4 , are the same, whereas the separations of $M_1 - BS$ (beam splitter), $M_3 - BS$ can be different. For the whole interferometer there are several basic modes to be considered:

- the input laser beam modes E_{mn} ;
- the basic FP-modes with
 - U_{mn} at M_1, M_3 ;
 - U'_{mn} at M_2, M_4 .
- the basic modes of the first recycling cavity $M_0 - BS - M_1$ (length d^R) with
 - V_{mn} at M_0 ;
 - V'_{mn} at M_1 .
- the basic modes of the second recycling cavity $M_0 - BS - M_3$ (length d^L) with
 - W_{mn} at M_0 ;
 - W'_{mn} at M_3 .

According to these definitions, each beam departing from the mirrors of Fig. 1, can be expressed as a linear superposition of the appropriate cavity modes, as follows:

$$\begin{aligned}\psi_i &= \sum_{m,n} C_{mn}^i E_{mn}, (i = 1, b) \\ \psi_2 &= \sum_{m,n} C_{mn}^2 V'_{mn}, & \psi_3 &= \sum_{m,n} C_{mn}^3 W'_{mn}, \\ \psi_j &= \sum_{k,l} C_{kl}^j U_{kl}, (j = 4, 6), & \psi_j &= \sum_{k,l} C_{kl}^j U'_{kl}, (j = 5, 7, 8, 9)\end{aligned}\quad (5)$$

Similarly the impinging beams can be written as :

$$\begin{aligned}\psi_{in} &= \sum_{m,n} C_{mn}^{in} E_{mn}, \\ \psi'_4 &= \int \int_{M_1} K^L(x, y; x', y') \psi_4 dx' dy' = \sum_{k,l} C_{kl}^4 b_{kl}^R U'_{kl}, & \psi'_5 &= \sum_{k,l} C_{kl}^5 b_{kl}^L U_{kl}, \\ \psi'_1 &= \sum_{m,n,i,j} T_B C_{ij}^1 C_{ij,mn}^{EV} p_{mn}^R V'_{mn}, & \psi'_6 &= \sum_{k,l} C_{kl}^6 b_{kl}^R U'_{kl}, \\ \psi'_3 &= \sum_{m,n,i,j} R_B C_{ij}^1 C_{ij,mn}^{EW} q_{mn}^R W'_{mn}, & \psi'_7 &= \sum_{k,l} C_{kl}^7 b_{kl}^L U_{kl}, \\ \psi'_2 &= \sum_{m,n,i,j} (T_B C_{ij}^2 p_{ij}^L C_{mn,ij}^{EV} + R_B C_{ij}^3 q_{ij}^L C_{ij,mn}^{EW}) E_{mn} \\ \psi_o &= \sum_{m,n} C_{mn}^o E_{mn} = \sum_{m,n,i,j} (T_B C_{ij}^3 q_{ij}^L C_{mn,ij}^{EW} - R_B C_{ij}^2 p_{ij}^L C_{mn,ij}^{EV}) E_{mn}\end{aligned}\quad (6)$$

where C_{mn}^i are the expansion coefficients of the beams and $C_{mn,ij}^{EV}$ and $C_{mn,ij}^{EW}$ are the mode conversion coefficients

$$C_{mn,ij}^{EV} = \int \int_{M_0} E_{mn}(x, y) V_{ij}(x, y) dx dy, \quad C_{mn,ij}^{EW} = \int \int_{M_0} E_{mn}(x, y) W_{ij}(x, y) dx dy \quad (7)$$

The round-trip eigenvalues are

$$\begin{aligned}b_{mn} &= b_{mn}^L b_{mn}^R, & b'_{mn} &= b_{mn}^L b_{mn}^R \\ p_{mn} &= p_{mn}^L p_{mn}^R, & q_{mn} &= q_{mn}^L q_{mn}^R\end{aligned}\quad (8)$$

where b_{mn} and b'_{mn} refer to the two FPs and p_{mn} and q_{mn} to the two recycling cavities.

From the linear combination of the electric field and Eq.(6) we can derive the following set of equations (the amplitude reflectivity from a dense to a rare medium has π phase shift)

$$\begin{aligned}\psi_1 &= T_0 \psi_{in} - R_0 \psi'_2, & \psi_2 &= T_1 \psi'_5 + R_1 \psi'_1 \\ \psi_3 &= T_1 \psi'_7 + R_1 \psi'_3, & \psi_4 &= T_1 \psi'_1 - R_1 \psi'_5 \\ \psi_5 &= -R_2 \psi'_4, & \psi_6 &= T_1 \psi'_3 - R_1 \psi'_7 \\ \psi_7 &= -R_2 \psi'_6, & \psi_8 &= T_2 \psi'_4 \\ \psi_9 &= T_2 \psi'_6, & \psi_b &= R_0 \psi_{in} + T_0 \psi'_2\end{aligned}\quad (9)$$

where $R_0, R_1, R_2, R_B, T_0, T_1, T_2$, and T_B are the amplitude reflectivity and the amplitude transmittivity of the mirrors $M_0, M_1(M_3), M_2(M_4)$, and beam splitter BS . By solving the set of Eqs(9) and using the definitions of Eq. (6) one has

$$\begin{aligned} C_{kl}^8 &= T_2 C_{kl}^4 b_{kl}^R, & C_{kl}^4 &= \frac{T_B T_1}{1 - R_1 R_2 b_{kl}} \sum_{i,j} C_{ij}^1 G_{ij,kl} \\ C_{kl}^9 &= T_2 C_{kl}^6 b_{kl}^R, & C_{kl}^6 &= \frac{R_B T_1}{1 - R_1 R_2 b_{kl}'} \sum_{i,j} C_{ij}^1 H_{ij,kl} \end{aligned} \quad (10)$$

where the coefficients $G_{ij,kl}$ and $H_{ij,mn}$ are given by

$$G_{ij,kl} = \sum_{m,n} C_{ij,mn}^{EV} p_{mn}^R C_{kl,mn}^{UV}, \quad H_{ij,kl} = \sum_{m,n} C_{ij,mn}^{EW} q_{mn}^R C_{kl,mn}^{UW} \quad (11)$$

and $C_{kl,mn}^{UV}, C_{kl,mn}^{UW}$ are the mode conversion factors

$$C_{kl,mn}^{UV} = \int \int_{M_1} U_{kl}(x, y) V'_{mn}(x, y) dx dy, \quad C_{kl,mn}^{UW} = \int \int_{M_3} U_{kl}(x, y) W'_{mn}(x, y) dx dy \quad (12)$$

The expressions for $C_{mn}^{1,b}$ are defined by the equations

$$\begin{aligned} C_{mn}^1 + R_0 \sum_{i,j} C_{ij}^1 [R_1 (T_B^2 C_{ij,mn} + R_B^2 D_{ij,mn}) - R_2 T_1^2 (T_B^2 E_{ij,mn} + R_B^2 F_{ij,mn})] &= T_0 C_{mn}^{in} \\ m, n &= 0, 1, 2, 3, 4, \dots \end{aligned} \quad (13)$$

where

$$\begin{aligned} C_{ij,mn} &= \sum_{k,l} C_{ij,kl}^{EV} p_{kl} C_{mn,kl}^{EV}, & D_{ij,mn} &= \sum_{k,l} C_{ij,kl}^{EW} q_{kl} C_{mn,kl}^{EW} \\ E_{ij,mn} &= \sum_{k,l} A_{ij,kl} p_{kl}^L C_{mn,kl}^{EV}, & F_{ij,mn} &= \sum_{k,l} B_{ij,kl} q_{kl}^L C_{mn,kl}^{EW} \end{aligned} \quad (14)$$

Finally, the expressions (5, 6) for the beam ψ_b, ψ_o, ψ_2 , and ψ_3 turn out to be determined by the following coefficients

$$\begin{aligned} C_{mn}^b &= R_0 C_{mn}^{in} + T_0 \sum_{i,j} (T_B C_{ij}^2 p_{ij}^L C_{mn,ij}^{EV} + R_B C_{ij}^3 q_{ij}^L C_{mn,ij}^{EW}) \\ C_{mn}^o &= \sum_{i,j} (T_B C_{ij}^3 q_{ij}^L C_{mn,ij}^{EW} - R_B C_{ij}^2 p_{ij}^L C_{mn,ij}^{EV}) \\ C_{mn}^2 &= \sum_{i,j} T_B C_{ij}^1 (R_1 C_{ij,mn}^{EV} p_{mn}^R - R_2 T_1^2 A_{ij,mn}) \\ C_{mn}^3 &= \sum_{i,j} R_B C_{ij}^1 (R_1 C_{ij,mn}^{EW} q_{mn}^R - R_2 T_1^2 B_{ij,mn}) \\ m, n &= 0, 1, 2, 3, 4, \dots \end{aligned} \quad (15)$$

where

$$A_{ij,mn} = \sum_{k,l} \frac{G_{ij,kl} b_{kl} C_{kl,mn}^{UV}}{1 - R_1 R_2 b_{kl}}, \quad B_{ij,mn} = \sum_{k,l} \frac{H_{ij,kl} b'_{kl} C_{kl,mn}^{UW}}{1 - R_1 R_2 b'_{kl}} \quad (16)$$

3 Output Beam

The output beam ψ_o from Eq.(6) can be rewritten as

$$\psi_o = \psi_{o1}(L') - \psi_{o2}(L) \quad (17)$$

where $\psi_{o1}(L')$ and $\psi_{o2}(L)$ are from the different arms and given by Eq.(6)

$$\psi_{o1}(L') = \sum_{mn,ij} T_B C_{ij}^3 q_{ij}^L C_{mn,ij}^{EW} E_{mn}, \quad \psi_{o2}(L) = \sum_{mn,ij} R_B C_{ij}^2 p_{ij}^L C_{mn,ij}^{EV} E_{mn} \quad (18)$$

Let's consider the characteristics of the output beam in two cases.

3.1 Without GW Signals

In this case, we have that $L' = L$. If the Michelson arms are not equal ($d^L \neq d^R$), but the difference $\delta d = d^R - d^L$ is not too large. It is reasonable to assume that $V_{mn} = W_{mn}$ and $V'_{mn} = W'_{mn}$. Then the output beam can be rewritten as

$$\begin{aligned} \psi_o(L) = & R_B T_B \sum_{mn} \sum_{\alpha\beta} C_{\alpha\beta}^1 [R_1 \sum_{ij} C_{mnij}^{EV} C_{\alpha\beta ij}^{EV} (q_{ij} - p_{ij}) \\ & - R_2 T_1^2 \sum_{ijkl\gamma\delta} \frac{C_{mnij}^{EV} C_{\alpha\beta\gamma\delta}^{EV} b_{kl} C_{kl ij}^{UV} C_{ij\gamma\delta}^{UV}}{1 - R_1 R_2 b_{kl}} (q_{ij}^L q_{\gamma\delta}^R - p_{ij}^L p_{\gamma\delta}^R)] E_{mn} \end{aligned} \quad (19)$$

where $b_{mn}(L)$, $p_{mn}(d)$ and $q_{mn}(d)$ are the eigenvalues of the two FP cavities and two recycling cavities given by (q_{mn} have the same forms as p_{mn})

$$\begin{aligned} b_{mn}(L) = & \exp[-i(2kL - (m+n+1)\arccos(2g-1))], \\ g = & 1 - \frac{L}{R}, \quad L = 3000m, \quad R = 3450m. \end{aligned} \quad (20)$$

and the $p_{mn}(d)$ are

$$\begin{aligned} p_{mn}(d) = & \exp[-i(2kd - (m+n+1)\arccos(2g'-1))], \\ g' = & 1 - \frac{d}{R'}, \quad d = 12m, \quad R' = 112512m. \end{aligned} \quad (21)$$

for plane-concave recycling cavities, and

$$\begin{aligned} p_{mn}(d) = & p_m p_n, \quad p_m = \exp[-s_m - i(kd + r_m)], \\ r_m = & -\frac{(m+1)^2 \pi}{16N}, \quad s_m = \frac{(m+1)^2}{8\sqrt{2}N^3}, \quad N(\text{Fresnel number}) = \frac{a^2}{\lambda L} \end{aligned} \quad (22)$$

for plane-parallel recycling cavities.

Dark Fringe and Background

If the Michelson arm lengths are equal ($d^L = d^R = d$), then $q_{ij}^L = p_{ij}^L, q_{ij}^R = p_{ij}^R$; one has

$$\psi_o = 0. \quad (23)$$

Therefore, no matter what kind of recycling cavities are used, as long as the Michelson arms are equal, the dark-fringe condition is always fulfilled.

If the Michelson arms are not equal ($d^L \neq d^R$), we usually have that

$$\psi_o \neq 0. \quad (24)$$

a background contribution will always present. This can be evaluated numerically.

If the two recycling cavities are 11.6m and 12.4m long, the background level that has been obtained for the plane-parallel and plano-concave cases are $1.18 \cdot 10^{-8} P_{in}$ and $6.25 \cdot 10^{-9} P_{in}$. These values are totally negligible with respect to the recycling power ($= 44 P_{in}$) of Eq.(32).

3.2 GW Signal Considered

If the GW signal is considered, we can assume that $L' = L_0 + \delta L$ and $L = L_0 - \delta L$, for small δL up to the first order we have that

$$\begin{aligned} \psi_{01}(L') &= \psi_{01}(L_0 + \delta L) \simeq \psi_{01}(L_0) + \frac{d\psi_{01}(L_0)}{dL} \delta L \\ &\simeq \psi_{01}(L_0) \left[1 + \frac{d\psi_{01}(L)/dL}{\psi_{01}(L_0)} \delta L \right] \simeq \psi_{01}(L_0) \exp\left[\frac{d\psi_{01}(L)/dL}{\psi_{01}(L_0)} \delta L \right] \\ &= \psi_{01}(L_0) e^{-i\Phi_{GW}} \\ \psi_{02}(L) &= \psi_{02}(L_0) e^{+i\Phi_{GW}} \quad \Phi_{GW} = \frac{d\psi_{01}(L)/dL}{\psi_{01}(L_0)} \delta L \end{aligned} \quad (25)$$

Then the output power is

$$\begin{aligned} P_{out} = |\psi_o|^2 &= |\psi_{01}(L_0)|^2 + |\psi_{02}(L_0)|^2 - 2\text{Re}[\psi_{01}^*(L_0)\psi_{02}(L_0)]\cos 2\Phi_{GW} \\ &\quad + 2\text{Im}[\psi_{01}^*(L_0)\psi_{02}(L_0)]\sin 2\Phi_{GW} \end{aligned} \quad (26)$$

Perfect Transverse Mode Match

If the Michelson interferometer is perfectly transverse mode matched, only the 00-mode survives. Then the output beam can be written as

$$\psi_{01}(L') = R_B T_B C_{00}^1 p_{00} R_F(L') E_{00}, \quad \psi_{02}(L) = R_B T_B C_{00}^1 p_{00} R_F(L) E_{00} \quad (27)$$

where R_F and C_{00}^1 can be deduced from Eqs.(15,13) and (14)

$$R_F(L) = \frac{R_1 - R_2 b_{00}(L)}{1 - R_1 R_2 b_{00}(L)}, \quad C_{00}^1 = \frac{T_0}{1 + R_0 R_F p_{00}(d)} \quad (28)$$

For small δL and up to the first order in δL we have that

$$\Phi_{GW} = 2kN_M\delta L \quad (29)$$

and

$$\begin{aligned} R_F(L') &\simeq R_F(L_0)\exp(-i2kN_M\delta L) \\ R_F(L) &\simeq R_F(L_0)\exp(+i2kN_M\delta L) \end{aligned} \quad (30)$$

If the FPs are on resonance, then

$$N_M = \frac{T_1^2 R_2}{(R_2 - R_1)(1 - R_1 R_2)} \quad (31)$$

From Eq.(26) the output power P_{out} can be rewritten as ($\delta L = \frac{1}{2}Lh$)

$$\begin{aligned} P_{out} &= 4|\psi_{01}(L_0)|^2 \sin^2 \Phi_{GW} = P_{in}|C_{00}^1|^2 R_F^2 \sin^2(2kN_M\delta L) \\ &= \frac{P_{in}}{2}|C_{00}^1|^2 R_F^2 [1 - \cos(2kN_M\delta L)] = P_{in}|C_{00}^1|^2 \left[\frac{T_1^2 R_2}{(1 - R_1 R_2)^2} kLh \right]^2 \end{aligned} \quad (32)$$

which is proportional to L^2 .

4 Phase Modulations

The longitudinal locking of the interferometer requires to phase-modulate the laser-beam. This offers the opportunity for an independent method to detect a GW-signal. In this chapter we will review this possibility.

4.1 Internal Modulation

In the so-called internal modulation a phase $\frac{1}{2}\delta\sin\Omega t$ is added to the light entering one arm, while simultaneously the same phase is subtracted from the light entering the other arm. This means that the phases entering Eqs.(30) become

$$\begin{aligned} 2kN_M L' &= 2kN_M L_0 + kN_M L_0 h + \frac{1}{2}\delta\sin\Omega t \\ 2kN_M L &= 2kN_M L_0 - kN_M L_0 h - \frac{1}{2}\delta\sin\Omega t \end{aligned} \quad (33)$$

and

$$\begin{aligned} 2kN_M\delta L &= 2kN_M(L' - L) = 2kN_M L_0 h + \delta\sin\Omega t \\ &= \Phi_0^{In} + \Phi_{GW} + \delta\sin\Omega t \end{aligned} \quad (34)$$

where Φ_0^{In} is an overall off-set phase. From Eq.(32). one has

$$P_{out}^{In} = 4|\psi_{01}(L_0)|^2 \frac{1}{2} [1 - \cos(\Phi_0^{In} + \Phi_{GW} + \delta\sin\Omega t)] \quad (35)$$

where Ω is the phase modulation frequency, Φ_{GW} is the GW signal. Eq.(35) can be reexpressed in the following way

$$P_{out}^{In} = 4|\psi_{o1}(L_0)|^2 \frac{1}{2} [1 - J_0(2\delta)\cos 2\Phi + 2J_1(2\delta)\sin 2\Phi \sin \Omega t - 2J_2(2\delta)\cos 2\Phi \cos 2\Omega t + \dots] \quad (36)$$

where $\Phi = \Phi_0^{In} + \Phi_{GW}$. For a small modulation depth δ and small Φ , Eq.(36) can be approximated as

$$P_{out}^{In} = P_{dc}^{In} + P_{\Omega}^{In} \sin \Omega t + P_{2\Omega}^{In} \cos 2\Omega t \\ = P_0 \frac{1}{2} [\delta^2 + 4\delta(\Phi_0^{In} + \Phi_{GW}) \sin \Omega t - \delta^2 \cos 2\Omega t + \dots] \quad (37)$$

$$P_0 = 4|\psi_{o1}(L_0)|^2 \quad (38)$$

4.2 Frontal Modulation

In the frontal modulation configuration the laser beam is phase-modulated at the input of the interferometer. The input beam may be written as $\psi_{in}[J_0(2\delta) + J_1(2\delta)\exp(i\Omega t) - J_1(2\delta)\exp(-i\Omega t)]$. The output beam becomes

$$\psi'_o = \psi_{o1}(L')[J_0 + J_1 e^{i\Omega t} e^{-i2\frac{\Omega}{c}d^L} - J_1 e^{-i\Omega t} e^{i2\frac{\Omega}{c}d^L}] \\ - \psi_{o2}(L)[J_0 + J_1 e^{i\Omega t} e^{-i2\frac{\Omega}{c}d^R} - J_1 e^{-i\Omega t} e^{i2\frac{\Omega}{c}d^R}] \\ = (\psi_{o1} - \psi_{o2})J_0 + i(\psi_{o1} - \psi_{o2})2J_1 \sin[\Omega t - \frac{\Omega}{c}(d^L + d^R)] \cos \frac{\Omega}{c}(d^L - d^R) \\ - i(\psi_{o1} + \psi_{o2})2J_1 \cos[\Omega t - \frac{\Omega}{c}(d^L + d^R)] \sin \frac{\Omega}{c}(d^L - d^R) \\ = J_0(\psi_{o1} - \psi_{o2}) + i2J_1[(\psi_{o1} - \psi_{o2})\sin \Psi \cos \Theta - (\psi_{o1} + \psi_{o2})\cos \Psi \sin \Theta] \quad (39)$$

where

$$\Psi = \Omega t - \frac{\Omega}{c}(d^L + d^R), \quad \Theta = \frac{\Omega}{c}(d^L - d^R) \quad (40)$$

Usually $d^L \neq d^R$, and we can show that

$$\psi_{o1} - \psi_{o2} = [\psi_{o1}(L_0) - \psi_{o2}(L_0)]\cos(\Phi_{GW}) - i[\psi_{o1}(L_0) + \psi_{o2}(L_0)]\sin(\Phi_{GW}) \\ \psi_{o1} + \psi_{o2} = [\psi_{o1}(L_0) + \psi_{o2}(L_0)]\cos(\Phi_{GW}) - i[\psi_{o1}(L_0) - \psi_{o2}(L_0)]\sin(\Phi_{GW}) \quad (41)$$

and the output power becomes

$$P_{out}^{Fr} = P_{dc}^{Fr} + P_{\Omega}^{Fr} \cos \Psi + P_{2c}^{Fr} \cos 2\Psi + P_{2s}^{Fr} \sin 2\Psi \quad (42)$$

where

$$P_{dc}^{Fr} = [|\psi_{o1}(L_0)|^2 + |\psi_{o2}(L_0)|^2](1 + \Phi_{GW}^2) + 4(J_0^2 + 2\delta^2 \cos 2\Theta) \text{Im}[\psi_{o1}^*(L_0)\psi_{o2}(L_0)]\Phi_{GW} \\ - 2(J_0^2 + 2\delta^2 \cos 2\Theta) \text{Re}[\psi_{o1}^*(L_0)\psi_{o2}(L_0)](1 - \Phi_{GW}^2) \quad (43)$$

$$P_{\Omega}^{Fr} = 4\delta \sin\Theta [2\text{Im}[\psi_{o1}^*(L_0)\psi_{o2}(L_0)](1 - \Phi_{GW}^2) - 4\text{Re}[\psi_{o1}^*(L_0)\psi_{o2}(L_0)]\Phi_{GW}] \quad (44)$$

$$P_{2c}^{Fr} = 2\delta^2[-(|\psi_{o1}(L_0)|^2 + |\psi_{o2}(L_0)|^2)\cos 2\Theta(1 + \Phi_{GW}^2) - 4\text{Im}[\psi_{o1}^*(L_0)\psi_{o2}(L_0)]\Phi_{GW} + 2\text{Re}[\psi_{o1}^*(L_0)\psi_{o2}(L_0)](1 - \Phi_{GW}^2)] \quad (45)$$

$$P_{2s}^{Fr} = -\delta^2[|\psi_{o1}(L_0)|^2 - |\psi_{o2}(L_0)|^2]\sin 2\Theta(1 + \Phi_{GW}^2) \quad (46)$$

The numerical results show that when the recycling cavity length difference is up to 0.8 meters

$$\frac{|\psi_{o1}(L_0)|^2 - \text{Re}[\psi_{o1}^*(L_0)\psi_{o2}(L_0)]}{|\psi_{o1}(L_0)|^2} < 10^{-9} \quad (47)$$

So the output power can be expressed as

$$P_{out}^{Fr} = P_{dc}^{Fr} + P_{\Omega}^{Fr} \cos\Psi + P_{2c}^{Fr} \cos 2\Psi + P_{2s}^{Fr} \sin 2\Psi \\ \simeq P_0[2\delta^2 \sin^2\Theta + 4\delta \sin\Theta(\Phi_0^{Fr} - \Phi_{GW})\cos\Psi + 2\delta^2 \sin^2\Theta \cos 2\Psi] \quad (48)$$

where $\Phi_{GW} \ll 1$, and

$$\Phi_0^{Fr} = \frac{\text{Im}[\psi_{o1}^*(L_0)\psi_{o2}(L_0)]}{2\text{Re}[\psi_{o1}^*(L_0)\psi_{o2}(L_0)]} \quad (49)$$

In the general case the output power is given by Eq.(42) with the help of Eq.(43,44,45,46,49).

In the special case where $d^L = d^R$ ($\psi_{o1}(L_0) = \psi_{o2}(L_0)$) one has

$$P_{out}^{Fr} = 4|\psi_{o1}(L_0)|^2 \Phi_{GW}^2 [1 - 2\delta^2 \cos 2[\Omega t - \frac{\Omega}{c}(d^L + d^R)]] \quad (50)$$

4.3 Some Results

The output beam ψ_o with frontal phase modulation can be written as

$$\psi_o' = \sum_{mn} C'_{mn} E_{mn} = \sum_{mn} (D_{mn}^0 + D_{mn}^1 e^{i\Omega t} + D_{mn}^2 e^{-i\Omega t}) E_{mn} \quad (51)$$

and the output power is

$$P_{out} = |\psi_o'|^2 = \sum_{mn} [|D_{mn}^0|^2 + |D_{mn}^1|^2 + |D_{mn}^2|^2 \\ + 2\text{Re}[D_{mn}^0(D_{mn}^1 + D_{mn}^2)]\cos\Omega t - 2\text{Im}[D_{mn}^0(D_{mn}^1 - D_{mn}^2)]\sin\Omega t \\ + 2\text{Re}(D_{mn}^{1*} D_{mn}^2)\cos 2\Omega t + 2\text{Im}(D_{mn}^{1*} D_{mn}^2)\sin 2\Omega t] \\ = P_{dc}' + P_{1c}' \cos\Omega t + P_{1s}' \sin\Omega t + P_{2c}' \cos 2\Omega t + P_{2s}' \sin 2\Omega t \quad (52)$$

Fig.2 shows the output given by Eq.(52) for the plane-concave recycling cavities, while the Fig.3 shows the same for a plane-parallel recycling cavities. Curve 2a) shows the term of $Am = \sqrt{(P_{1c}')^2 + (P_{1s}')^2}$; 2b) shows the term of $Ph = \arctan(\frac{P_{1s}'}{P_{1c}'})$. These results are calculated with a modulation frequency of $\Omega = 6.2678\text{MHz}$, $d^R = 12.4\text{m}$ and $d^L = 11.6\text{m}$.

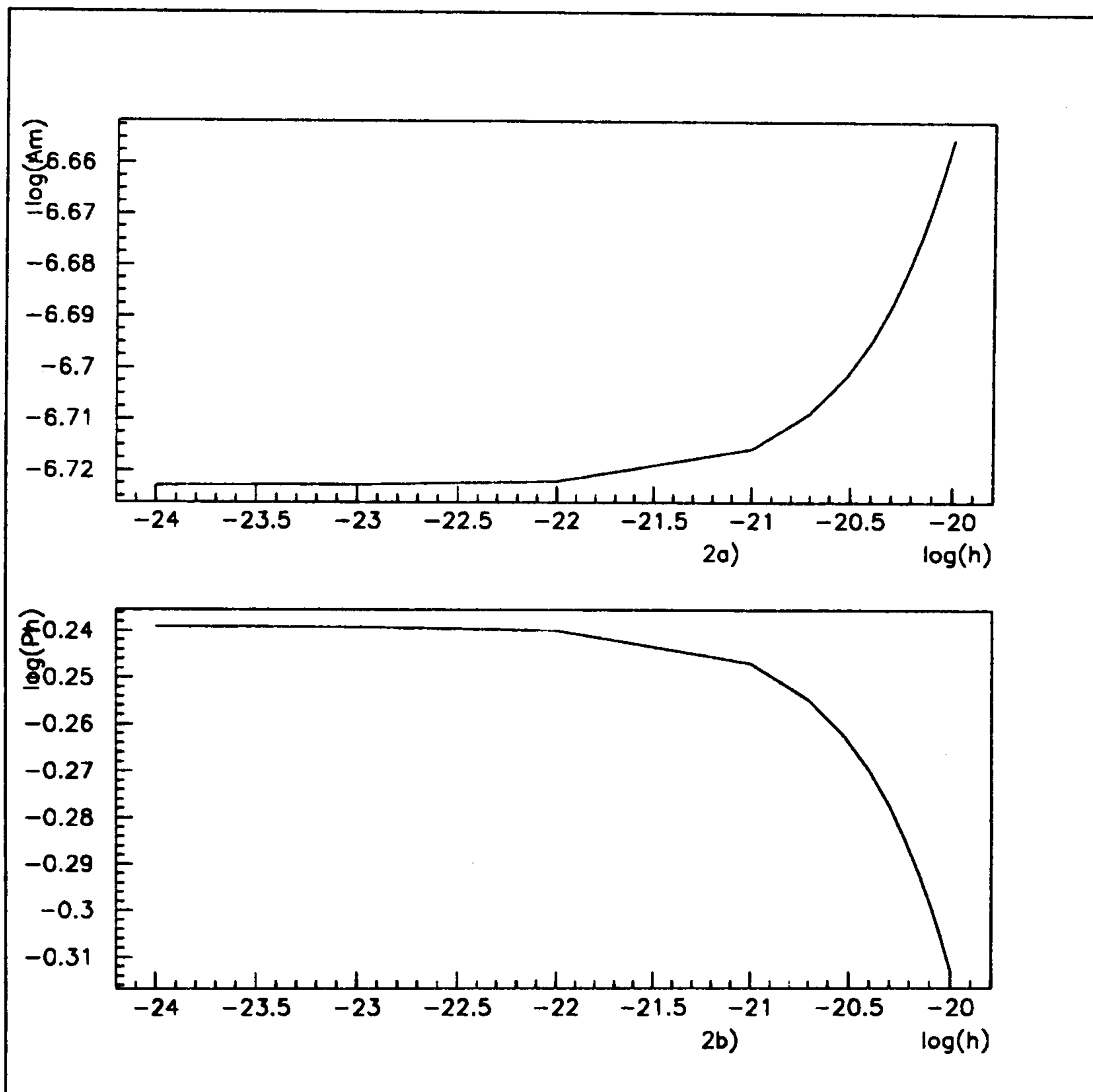


Figure 2: The amplitude and phase of the modulation frequency term with plano- concave recycling cavities (where Am and Ph are defined in text)

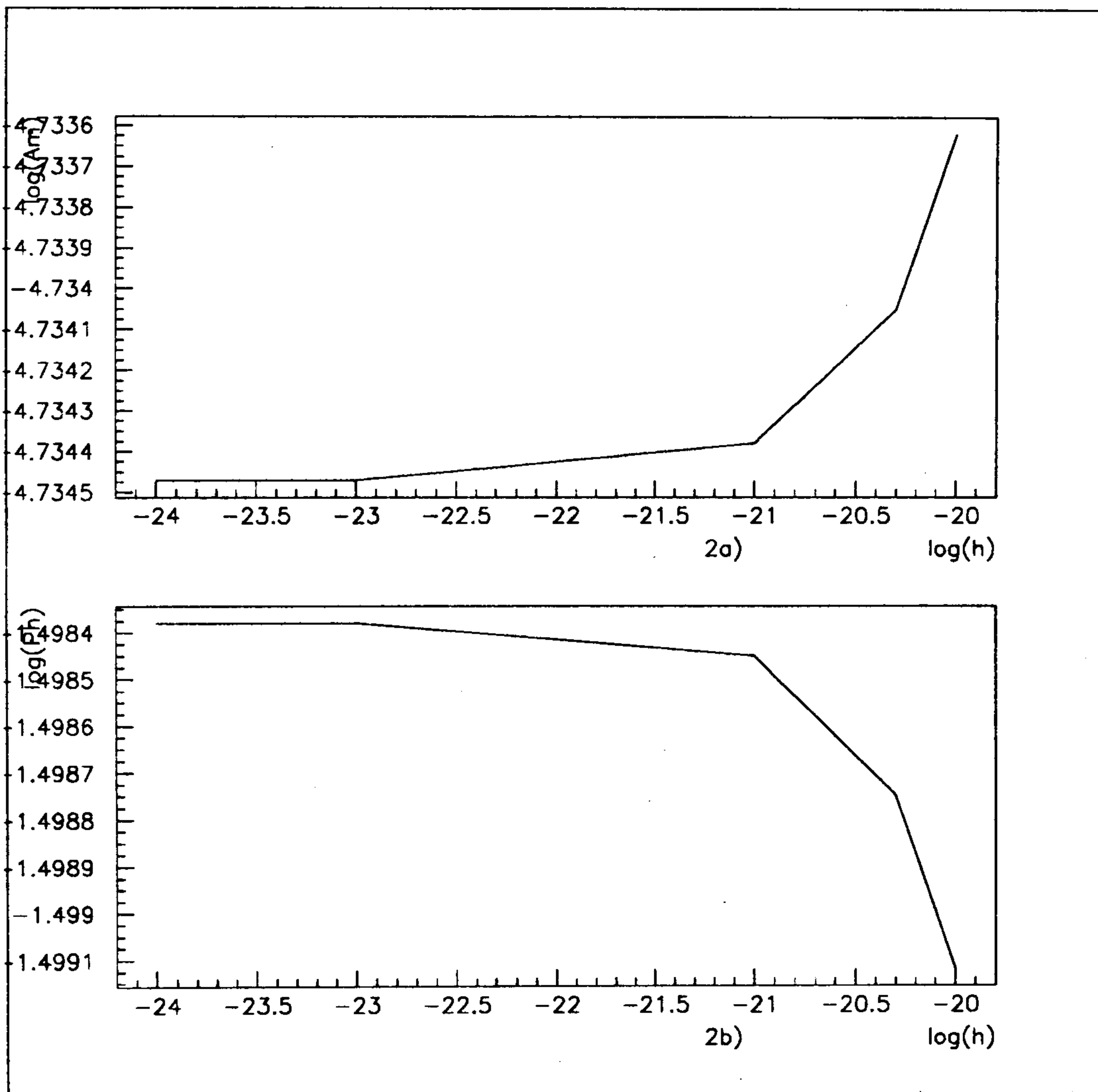


Figure 3: The amplitude and phase of the modulation frequency term with plane- parallel recycling cavities (where A_m and P_h are defined in text)

It is interesting to compare the output power at the detector without phase modulation, given by Eq.(32), and the demodulated power at the detector given by Eq.(37, 42) (both Φ_0^{In} and Φ_0^{Fr} are assumed to be zero),

$$\begin{aligned} P_{out} &= P_0 \Phi_{GW} \Phi_{GW} && \text{without - modulation} \\ P_{\Omega}^{In} &= 2P_0 \Phi_{GW} \delta && \text{internal - modulation} \\ P_{\Omega}^{Fr} &= 4P_0 \Phi_{GW} \delta \sin\Theta && \text{frontal - modulation} \\ P_0 &= 4|\psi_{01}(L_0)|^2 = P_{in} |C_{00}^1|^2 R_F^2 \end{aligned} \quad (53)$$

In VIRGO one has: $|C_{00}^1|^2 = 44.6$ and R_F^2 is close to 1. The demodulated output power with internal-phase modulation is $2\delta/\Phi_{GW}$ times larger than the output power without modulation. The demodulated output power with the frontal-phase modulation is lower than that of the internal-phase modulation scheme by a factor $2\sin\Theta$ ($\sin\Theta = 0.0126$ for the VIRGO case).

4.4 Photon Shot Noise

The "shot noise limited" value of h is determined by the photon statistics. In the case without modulation, the output power on the detector is given by Eq.(32).

$$P_{out} = P_0 \sin^2 \psi \quad (54)$$

where ψ is an off-set phase between the arms of the interferometer.

The shot noise associated to this power is

$$\Delta P_{out} = \sqrt{2P_0 \hbar \omega} \sin \psi \quad (55)$$

and the minimal phase variation that can be appreciated is given by

$$\delta \psi \geq \frac{\Delta P_{out}}{\frac{dP_{out}}{d\psi}} = \sqrt{\frac{\hbar \omega}{2P_0}} \frac{1}{\cos \psi} \quad (56)$$

That is to say that the best sensitivity is obtained when working on the "dark fringe" condition $\psi = 0$. Since a GW induces the dephasing given by Eq.(29, 31), The shot noise limited value of h is given by

$$h_{shot-noise} \geq \frac{1}{kLN_M} \sqrt{\frac{\hbar \omega}{2P_0}} \quad (57)$$

where P_0 is given by Eq.(53). Eqs.(32, 57) show that the shorter the length L and the worse the h -sensitivity is. When the arms are different the shot noise limited h value does not change much,

$$\frac{h_{shot-noise-equal-arms} - h_{shot-noise-unequal-arms}}{h_{shot-noise-unequal-arms}} < 7.65 * 10^{-7} \quad (58)$$

For a 20 watt input laser beam (P_{in}) the minimum detectable value for h is $1.81 * 10^{-23} / \sqrt{Hz}$.

With a similar argument, the 'shot noise' limited value of h can be obtained in the case of phase modulation.

For the internal modulation Eq.(37) gives the average power impinging upon the detector

$$\langle P \rangle = \frac{1}{2} P_0 \delta^2 \quad (59)$$

which is affected by the shot noise

$$\Delta P = \sqrt{2 \frac{1}{2} P_0 \delta^2 \hbar \omega} = \sqrt{P_0 \delta^2 \hbar \omega} \quad (60)$$

By demodulating the signal one can isolate the $\sin \Omega t$ component P_Ω . Therefore the minimal phase variation again is given by

$$\delta \psi \geq \frac{\Delta P}{\frac{dP_\Omega}{d\psi}} = \frac{\sqrt{P_0 \delta^2 \hbar \omega}}{2 P_0 \delta} = \frac{1}{2} \sqrt{\frac{\hbar \omega}{P_0}} \quad (61)$$

and for h one has

$$h_{shot} \geq \frac{1}{\sqrt{2kLN_M}} \sqrt{\frac{\hbar \omega}{2P_0}} \quad (62)$$

Finally for the frontal modulation the result turns out to be exactly the same.

5 Discussions

The performances of the plane-parallel recycling cavities and plano-concave recycling cavities will now be compared.

5.1 Non-Modulated Interferometer

First, we assumed that the arm lengths of the Michelson and the cavity length of FPs are the same. The numerical results of the two cases have no differences.

Second, we discuss the case of the Michelson with different arm lengths. If the two arms are 12.4 and 11.6 meter long, we list the performances of the two cases in Table I.

Table I

Recycling Cavities	Plane-Parallel	Plano-Concave
Total Recycling Power ($in P_{in}$)	44.582	44.582
00-Mode Recycling Power	44.582	44.582
FP Intracavity Power ($in P_{in}$)	709.23	709.25
00-Mode Intracavity Power	709.23	709.25
Reflected Power ($in P_{in}$)	0.8581	0.8581
The Background in (P_{in})	$0.118 * 10^{-7}$	$0.625 * 10^{-8}$

In both cases the dark fringe condition is not satisfied, the output back ground are $0.625 * 10^{-8} P_{in}$ and $1.18 * 10^{-8} P_{in}$ respectively, which are much higher than the shot noise limited detectable signal power. The output power due to the GW signal of the shot noise limited value of $h = 1.81 * 10^{-23}$ is $0.873 * 10^{-16} P_{in}$ for plano-concave recycling cavities; and $0.695 * 10^{-14} P_{in}$ for plane- parallel recyclings. This requires that the input laser beam power fluctuation must be less than $\frac{0.873 * 10^{-16} P_{in}}{0.625 * 10^{-8} P_{in}} \simeq 1.4 * 10^{-8}$ for plano-concave and $\frac{0.695 * 10^{-14} P_{in}}{1.18 * 10^{-8} P_{in}} \simeq 5.9 * 10^{-7}$ for plane-parallel recyclings.

Since these requirements are difficult to achieve at low frequencies, phase modulation appears to be necessary.

For plane-concave recycling cavities the sensitivity of the performances of the interferometer on the radius of curvature of mirror M_0 is shown in Table II.

Table II

r_{M_0}	110000m	112000m	112512m	113000m	120000m
relative difference of recycling power for $d^R = d^L$	$3.06 * 10^{-5}$	$1.26 * 10^{-6}$	0.0	$1.12 * 10^{-6}$	$2.49 * 10^{-4}$
relative difference of recycling power for $d^R \neq d^L$	$3.06 * 10^{-5}$	$1.25 * 10^{-6}$	$1.51 * 10^{-15}$	$1.12 * 10^{-6}$	$2.49 * 10^{-4}$

In the Table r_{M_0} is the radius of curvature of the mirror M_0 . The perfectly transverse mode matched value of r_{M_0} is 112512.00m. If the Michelson arm lengths are the same, while the radius of curvature of mirror M_0 varies from 110000m to 120000m, the relative difference of FP power (the difference between the total power in FP and the power in 00 mode over the total power) is less than 10^{-8} . For the recycling powers the relative differences are shown in Table II. For the different arm length Michelson (11.6m, 12.4m), the relative differences of FP powers are the same as the equal arm length case. The relative differences of recycling powers are also shown in Table II. The Table shows that, if the radius of curvature r_{M_0} is accurate to the level of 0.1 percent, the performance of the interferometer does not change much.

5.2 With Phase Modulation

Table III presents the results obtained with the phase modulation with the same conditions of Table I.

We see that the background in the modulation frequency term is still much higher than the GW signal. For plane- parallel recycling cavities the background is two orders of magnitude higher than the one of plano-concave recycling cavities. With this background the detection of the shot noise limited value of h , requires the laser beam power fluctuations to be less than $5.43 * 10^{-6}$ for plane-parallel recyclings, and $3.54 * 10^{-4}$ for plano-concave recycling cavities.

Table III

	$P_{dc}^{Fr}(P_{in})$	$ P_{\Omega}^{Fr} (P_{in})$	$arg[P_{\Omega}^{Fr}]$
Plano-Concave recycling cavity with no GW signal	0.03244	$1.89270 * 10^{-7}$	$-.57657rad.$
with GW signal	0.03244	$1.89326 * 10^{-7}$	$-.57638rad.$
the effect of GW	0.0	$0.6701 * 10^{-10}$	$-.01492rad.$
Plane-Parallel recycling cavity with no GW signal	0.03151	$1.84303 * 10^{-5}$	$-.03174rad.$
with GW signal	0.03151	$1.84304 * 10^{-5}$	$-.03174rad.$
the effect of GW	0.0	$1.0000 * 10^{-10}$	$-.01000rad.$

References

- [1] J. Y. Vinet, J. Phys., 47(1986), 639.
- [2] J. Y. Vinet, B. J. Meers, Phys. Rev. D, 38(1988), 433.
- [3] B. J. Meers, Phys. Rev. D, 38(1988), 2317.
- [4] B. J. Meers, Phys. Lett. A, 142(1989), 465.
- [5] H. Kogelnik, and T. Li, Appl. Opt. 5(1966), 1550.